

HEMATOPOIESIS AND STEM CELLS

FGF-23 from erythroblasts promotes hematopoietic progenitor mobilization

Shinichi Ishii,¹ Tomohide Suzuki,¹ Kanako Wakahashi,¹ Noboru Asada,¹ Yuko Kawano,¹ Hiroki Kawano,¹ Akiko Sada,¹ Kentaro Minagawa,¹ Yukio Nakamura,² Seiya Mizuno,³ Satoru Takahashi,³⁻⁶ Toshimitsu Matsui,⁷ and Yoshio Katayama¹

¹Division of Hematology, Department of Medicine, Kobe University Graduate School of Medicine, Kobe, Japan; ²Cell Engineering Division, RIKEN BioResource Research Center, Ibaraki, Japan; ³Transborder Medical Research Center (TMRC), ⁴Department of Anatomy and Embryology, Faculty of Medicine, ⁵International Institute for Integrative Sleep Medicine (WPI-IIS), and ⁶Life Science Center, Tsukuba Advanced Research Alliance (TARA), University of Tsukuba, Tsukuba, Japan; and ⁷Department of Hematology, Nishiwaki Municipal Hospital, Nishiwaki, Japan

KEY POINTS

- Bone marrow FGF-23 from erythroblasts promotes G-CSF-induced progenitor mobilization.
- FGF-23 interferes with the chemoattraction of progenitors toward CXCL-12.

Fibroblast growth factor 23 (FGF-23) hormone is produced by bone-embedded osteocytes and regulates phosphate homeostasis in kidneys. We found that administration of granulocyte colony-stimulating factor (G-CSF) to mice induced a rapid, substantial increase in FGF-23 messenger RNA in bone marrow (BM) cells. This increase originated mainly from CD45⁺Ter119⁺CD71⁺ erythroblasts. FGF-23 protein in BM extracellular fluid was markedly increased during G-CSF-induced hematopoietic progenitor cell (HPC) mobilization, but remained stable in the blood, with no change in the phosphate level. Consistent with the BM hypoxia induced by G-CSF, low oxygen concentration induced FGF-23 release from human erythroblast HUDEP-2 cells in vitro. The efficient mobilization induced by G-CSF decreased drastically in both FGF-23^{-/-} and chimeric mice with FGF-23 deficiency, only in hematopoietic cells, but increased in osteocyte-specific FGF-23^{-/-} mice. This finding suggests that erythroblast-derived, but not bone-derived, FGF-23 is needed to release

HPCs from BM into the circulation. Mechanistically, FGF-23 did not influence CXCL-12 binding to CXCR-4 on progenitors but interfered with their transwell migration toward CXCL-12, which was canceled by FGF receptor inhibitors. These results suggest that BM erythroblasts facilitate G-CSF-induced HPC mobilization via FGF-23 production as an intrinsic suppressor of chemoattraction. (*Blood*. 2021;137(11):1457-1467)

Introduction

Granulocyte colony-stimulating factor (G-CSF) is clinically used for hematopoietic stem/progenitor cell (HSC/HPC) mobilization from the bone marrow (BM) into the circulation. G-CSF stimulation and subsequent marrow hypersympathetic tone suppress the hematopoietic microenvironment, such as osteolineage cells,¹⁻⁵ mesenchymal stem cells,⁶ and macrophages,⁷⁻⁹ resulting in the release of HSCs/HPCs from the BM. However, the mechanism for mobilization is still unclear. The contribution of the CXCR-4/CXCL-12 axis in this process is not fully understood. Although the CXCL-12 protein level in BM extracellular fluid is drastically decreased, probably because of osteoblast suppression and increased protease activity,^{2,10-12} total CXCL-12 expression in CXCL-12-abundant reticular (CAR) cells is only minimally affected by G-CSF.¹³ A CXCR-4 antagonist, plerixafor, is also clinically applied to facilitate G-CSF mobilization, particularly in patients with poor mobilization efficiency (eg, multiple myeloma).¹⁴ There may be an unknown mechanism to counteract the function of CXCR-4, rather than CXCL-12 downregulation in BM, during G-CSF mobilization.

During our study on the role of a calcium-regulating hormone (vitamin D) in mobilization,³ we noted a strong induction, not

only in bone tissue, but also in BM cells, of another major mineral (phosphate)-regulating hormone, fibroblast growth factor 23 (FGF-23). FGF-23 is known to be mainly produced by bone-embedded osteocytes and, together with an FGF receptor (FGFR) coreceptor α -klotho, regulates phosphate homeostasis in the kidneys.¹⁵ However, the strong induction of FGF-23 in the local tissue and its unique function is unknown.

In this study, we showed that FGF-23 is dramatically increased in BM, mainly by erythroblasts during G-CSF treatment, and promotes HPC mobilization by inhibiting CXCR-4-mediated chemoattraction.

Methods

Mice for the experiments

Mice were under the husbandry care of the Institute for Experimental Animals, Kobe University Graduate School of Medicine. FGF-23^{-/-} and FGF-23^{lox/lox} mice were generated on a C57BL/6 background, as described in the supplemental Methods (available on the *Blood* Web site). DMP-1-cre mice were generated, as described previously,¹⁶ backcrossed onto a C57BL/6

background for >10 generations, and crossed with FGF-23^{flox/flox} mice to generate mice with conditional FGF-23 deletion in osteocytes. C57BL/6 mice were purchased from CLEA Japan (Chiba, Japan) 1 to 2 weeks before the experiments. C57BL/6-CD45.1 congenic mice were purchased from The Jackson Laboratory (Bar Harbor, ME). Animals were maintained under specific pathogen-free conditions in a 12-hour light/12-hour dark cycle. All mice were used at 7 to 8 weeks of age, except for experiments with FGF-23^{+/+} and FGF-23^{-/-} mice, for which 5-week-old littermates were used. Male mice were used in all experiments, except for the characterization of FGF-23^{-/-} mice (supplemental Figures 5-11) and transplant donors for BM chimera (see Figure 5; supplemental Figures 12-13 and 15), for which female FGF-23^{+/+} and FGF-23^{-/-} littermates were also used in some experiments. All animal studies were approved by the Animal Care and Use Committee of Kobe University.

G-CSF mobilization and isoproterenol treatment

HPC mobilization by G-CSF was induced, as described previously.³ In brief, mice were injected with recombinant human G-CSF (filgrastim; kindly provided by Kyowa Kirin, Tokyo, Japan; 125 µg/kg per dose every 12 hours in 8 divided doses, administered subcutaneously) in phosphate-buffered saline (PBS) supplemented with 0.1% bovine serum albumin (PBS/BSA). Blood and BM were harvested 3 hours after the last dose of G-CSF, unless otherwise indicated.

Treatment with single-dose isoproterenol (DL-isoproterenol hydrochloride, 100 mg/kg, administered intraperitoneally; Sigma-Aldrich, St Louis, MO) was performed as described previously.³ BM was harvested at time points established in the protocol.

Competitive repopulation assay

The stem cell activities of blood mobilized by G-CSF were assessed by long-term competitive reconstitution, as described previously,³ with minor modifications. In brief, 150 µL mobilized blood (CD45.2), together with 2×10^5 BM nucleated cells from a CD45.1 competitor donor, was injected into lethally irradiated (14 Gy, split dose) CD45.1-recipient mice. The proportion of peripheral blood leukocytes bearing CD45.1 or CD45.2 antigen was determined monthly after transplantation by flow cytometry. Repopulating units (RUs) were calculated by using the following standard formula: $RUs = \%(C)/(100 - \%)$, where % is the measured percentage of donor cells (CD45.2⁺ cells derived from mobilized blood), and C is the number of competitor marrow cells per 10^5 , which was 2 in this study.

ELISA for FGF-23 and CXCL-12

For the enzyme-linked immunosorbent assays (ELISAs), BM extracellular fluid was obtained by flushing femoral BM with 500 µL PBS, followed by centrifugation after several pipetting steps. FGF-23 quantification in serum, BM extracellular fluid, culture supernatants, and cell lysates was performed with an FGF-23 ELISA kit for mouse/human intact FGF-23 (iFGF-23; Kainos Laboratories, Tokyo, Japan) and an FGF-23 ELISA kit for mouse/rat C-terminal FGF-23 (cFGF-23; Immotopics, San Clemente, CA) according to the manufacturers' recommendations. CXCL-12 in BM extracellular fluid was evaluated with a CXCL-12 ELISA kit (R&D Systems, Minneapolis, MN).

Flow cytometry and cell sorting

The reagents for flow cytometry, including the antibodies PE anti-mouse CD45, biotin anti-mouse lineage panel (CD11b, Gr-1, Ter119, CD3e, and B220), FITC anti-mouse Sca-1, PE anti-mouse Sca-1, FITC anti-mouse c-kit, PE anti-mouse c-kit, APC anti-mouse c-kit, APC anti-mouse CXCR-4, PerCP/Cy5.5 anti-mouse CD8a, and FITC anti-mouse CD48 were from BD Pharmingen (San Diego, CA). FITC anti-mouse CD71, PerCP streptavidin, PerCP/Cy5.5 anti-mouse Ter119, PerCP/Cy5.5 anti-mouse CD45R/B220, PerCP/Cy5.5 anti-mouse Ly-6G/Ly-6C (Gr-1), PerCP/Cy5.5 anti-mouse CD11b, PerCP/Cy5.5 anti-mouse CD4, BV421 anti-mouse Sca-1, PE anti-mouse CD127, APC/Cy7 anti-mouse CD16/32, PE/Cy7 anti-mouse Sca-1, PE anti-mouse CD135, BV421 anti-mouse CD150, PE anti-mouse CD45R/B220, and PE anti-mouse CD3e were from BioLegend (San Diego, CA). FITC anti-mouse CD34, PE/Cy5 streptavidin, and APC/eFluor780 streptavidin were from eBioscience (San Diego, CA). FITC anti-mouse IgM was from SouthernBiotech (Birmingham, AL). Cells were suspended in 0.5% BSA/2 mM EDTA/PBS. Cell analyses were performed on a FACScan, Accuri C6 (BD Biosciences, San Jose, CA) or a CytoFLEX S flow cytometer (Beckman Coulter, Brea, CA). Data analysis was performed with FlowJo (Ashland, OR).

BM mononuclear cells (MNCs) were obtained by density gradient centrifugation of Lympholyte-M (Cedarlane, Burlington, ON, Canada) and CD45⁺ cells, CD45⁻Ter119⁺CD71⁺ erythroblasts, and CD45⁻Ter119⁻ nonhematopoietic (stromal) cells were sorted using the MoFlo XDP flow cytometer with Summit software (Beckman Coulter, Brea, CA).

HUDEP-2 culture

The human umbilical cord blood-derived erythroid progenitor cell line HUDEP-2 was generated as described previously.¹⁷ HUDEP-2 cells were cultured in serum-free medium for expansion of hematopoietic cells (STEMCELL Technologies, Vancouver, BC, Canada) supplemented with 50 ng/mL human stem cell factor (R&D Systems), 3 IU/mL human erythropoietin (epoetin-α [epo-α]; kindly provided by Kyowa Kirin), 1 µg/mL doxycycline (Sigma-Aldrich), and 10^{-6} M dexamethasone (Sigma-Aldrich) in a 24-well nonculture treatment plate (Falcon; Corning, Corning, NY) at 1×10^7 cells per 500 µL per well. After incubation in 21% and 5% O₂ conditions with 5% CO₂ at 37°C for 4 hours, the supernatants were used for FGF-23 ELISA.

Cell lysates

Sorted erythroblasts were lysed in a buffer containing 50 mM Tris-HCl (pH 7.5), 150 mM NaCl, 1% Triton X-100 (Wako, Osaka, Japan), 0.2 M sodium orthovanadate (Sigma-Aldrich), 0.2 M phenylmethylsulfonyl fluoride (Sigma-Aldrich), 1 M sodium fluoride (Nacalai Tesque, Kyoto, Japan), and protease inhibitor cocktail (Sigma-Aldrich). After centrifugation, the supernatants were directly used for FGF-23 ELISA.

Transwell migration

BM MNCs in Iscove's modified Dulbecco's medium (IMDM) supplemented with 2% fetal bovine serum (FBS; 1×10^6 cells per 100 µL) were added to the upper chamber of a transwell insert (pore size 5 µm; Corning). They migrated into the lower chamber, which contained 600 µL IMDM/2% FBS with 300 ng/mL mouse CXCL-12 (R&D Systems) in a 24-well nonculture treatment plate (Falcon), at 37°C, 5% CO₂. Various combinations of 3 µg/mL mouse FGF-23 (R&D Systems), 3 µg/mL mouse α-klotho (R&D

Systems), and 10 $\mu\text{g/mL}$ heparin (STEMCELL Technologies) were added to the upper or lower chamber. After 4 hours, the migration efficiency of the HPCs was evaluated by an assay of colony-forming unit cells (CFU-Cs) in a culture of input cells without loading into the transwell chamber and cells in the lower chamber.

To assess the effect of FGFR antagonists, the cells were incubated with 10 nM BGJ-398 (infigratinib; ChemScene, Monmouth Junction, NJ) or 10 nM JNJ-42756493 (erdafitinib; Cayman Chemical, Ann Arbor, MI) starting at 30 minutes before the transwell migration assay.

Binding assay of fluorochrome-conjugated CXCL-12

BM MNCs were incubated in IMDM/2% FBS for 2 hours, with or without FGF-23_{comb} (3 $\mu\text{g/mL}$ mouse FGF-23 [R&D Systems]+3 $\mu\text{g/mL}$ mouse α -klotho [R&D Systems]+10 $\mu\text{g/mL}$ heparin [STEMCELL Technologies]), and 20 μM Alexa647-conjugated mouse CXCL-12 (Almac, Nr Penicuik, United Kingdom) was added for the last 30 minutes of the period. Cells were stained with PE anti-Sca-1, FITC anti-c-kit, and biotin lineage panel, followed by PerCP streptavidin. CXCL-12 binding to lineage⁺Sca-1⁺c-kit⁺ cells was analyzed by flow cytometry. As a control for this experiment, cells without FGF-23_{comb} were incubated with mouse CXCL-12 (nonfluorescent, 300 ng/mL; R&D Systems), starting 30 minutes before the addition of Alexa647-conjugated mouse CXCL-12.

Actin polymerization

Actin polymerization in HPCs was assessed as described previously,¹⁸ with minor modifications. In brief, BM MNCs (2×10^6 cells per 100 μL PBS) were stimulated with 500 ng/mL mouse CXCL-12 (R&D Systems) for the indicated seconds, fixed, and permeabilized with BD Cytotfix/Cytoperm Fixation/Permeabilization Kit (BD Biosciences), according to the manufacturer's recommendations. The cells were stained with 3 U/mL Alexa488-conjugated phalloidin (Invitrogen, Carlsbad, CA) for 1 hour and further stained with APC anti-c-kit and a biotin lineage panel, followed by PerCP streptavidin. Actin polymerization in lineage⁺c-kit⁺ cells was analyzed by flow cytometry.

Statistical analysis

All data were pooled from at least 3 independent experiments, except those shown in supplemental Figure 16E, where data were from 2 experiments. All center values shown in the graphs refer to the mean. All values were reported as the mean \pm standard error of the mean (SEM). Statistical analysis was conducted with the 2-tailed, unpaired Student *t* test, Mann-Whitney *U* test, and 1-way analysis of variance (ANOVA) with Tukey's post hoc test. No samples or animals were excluded from the analysis. The animals were randomly assigned to groups. Statistical significance was assessed with Prism (GraphPad Software, San Diego, CA) and defined as $P < .05$.

Complete descriptions of other procedures (generation of FGF-23^{-/-} and FGF-23^{lox/lox} mice, generation of chimeric mice, blood biochemistries, RNA extraction and quantitative reverse transcription-polymerase chain reaction, bone histomorphometry, and pimonidazole staining) are provided in the supplemental Methods.

Results

FGF-23 is induced in BM cells during G-CSF–induced mobilization

FGF-23 messenger RNA (mRNA) in bone tissue was increased during G-CSF mobilization (every 12 hours for 8 doses; Figure 1A) and after a short time (1 hour) by single-dose G-CSF (Figure 1B). Although FGF-23 is known as a bone-derived hormone, BM cells similarly showed a sharp increase in FGF-23 mRNA (Figure 1C). Because G-CSF is a strong inducer of the sympathetic nervous system (SNS) signals,¹⁻⁵ FGF-23 mRNA induction in BM cells was examined by using a single-dose α -adrenergic receptor agonist isoproterenol, displaying similar or even stronger induction of FGF-23 mRNA (Figure 1D). A rapid (2 hours) increase in intact FGF-23 (iFGF-23) protein was observed in BM extracellular fluid (BM flushed from 1 femur with 500 μL PBS) and was maintained for 12 hours by single-dose G-CSF (Figure 2A). Alteration of the iFGF-23 protein level in BM extracellular fluid was assessed during G-CSF mobilization. Without G-CSF, most of the mice showed lower than detectable levels by ELISA. The level increased with the number of G-CSF doses, which peaked at 6 (Figure 2B), but remained stable in the blood with unchanged phosphate levels during G-CSF mobilization (Figure 2C-D). A rough estimation of the actual iFGF-23 concentration in the BM extracellular cavity during G-CSF mobilization (supplemental Figure 1) was extremely high (~ 1 -3 $\mu\text{g/mL}$; $\sim 20,000$ times higher than levels in the blood). Thus, FGF-23 is a G-CSF–inducible local factor in BM.

To assess the processing of the FGF-23 protein, iFGF-23 and C-terminal FGF-23 (cFGF-23 [iFGF-23+processed C-terminal FGF-23 fragment]) were measured in serum and BM extracellular fluid at 6 doses of PBS/BSA or G-CSF. As shown in Figure 2E, G-CSF treatment did not alter the iFGF-23 level, whereas cFGF-23 was clearly increased in the circulation. In BM extracellular fluid, most of the increased FGF-23 protein was iFGF-23, but the C-terminal FGF-23 fragment was most likely also increased (Figure 2E). These results suggest that a portion of the increased FGF-23 in BM was cleaved and that only the processed C-terminal FGF-23 fragment goes through the marrow-blood barrier during G-CSF treatment.

Erythroblasts produce FGF-23

FGF-23 mRNA was induced in the sorted CD45⁺, but not CD45⁻, cell population using single-dose G-CSF (Figure 3A) and isoproterenol (Figure 3B). Most of the CD45⁺ BM cells were Ter119⁺ erythroid lineage cells (the ratio of CD45⁺Ter119⁺CD71⁺ erythroblasts to CD45⁺Ter119⁻ nonhematopoietic [stromal] cells was $\sim 7:1$ [supplemental Figure 2]). These cells were sorted by using single-dose G-CSF or isoproterenol. FGF-23 mRNA was strongly induced in both erythroblasts and stromal cells (Figure 3C). CD45⁺Ter119⁺CD71⁺ erythroblasts were also sorted using single-dose G-CSF; cell lysates contained an increased iFGF-23 protein level similar to that obtained with single-dose isoproterenol (Figure 3D). Because these data were almost equivalent to cFGF-23 levels (Figure 3E), erythroblasts most likely produced iFGF-23 without a major contribution to its cleavage during G-CSF treatment.

To identify the possible triggering signal for secretion of FGF-23 from erythroblasts, we used the human erythroblast cell line HUDEP-2.¹⁷ HUDEP-2 incubation with various G-CSF or isoproterenol concentrations resulted in the no iFGF-23 protein

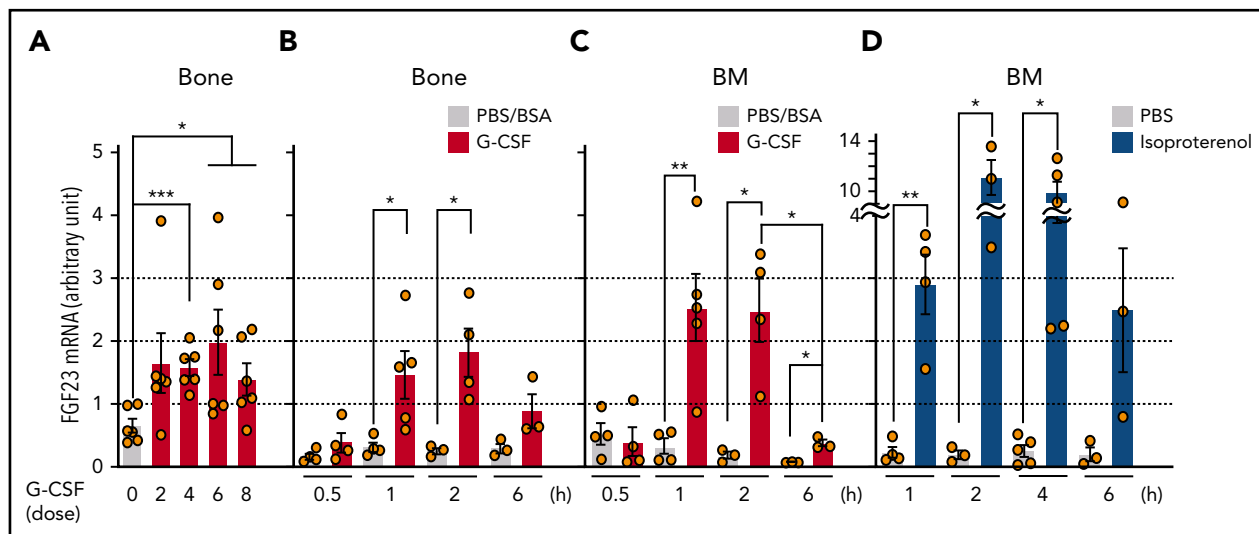


Figure 1. Expression of FGF-23 mRNA in bone and BM. (A-B) FGF-23 mRNA in bone tissue during G-CSF mobilization (A) (every 12 hours for 8 doses, harvested at 3 hours after each dose, $n = 6$) and after single-dose G-CSF (B) at the indicated hours ($n = 3-5$). (C-D) FGF-23 mRNA in BM cells after single-dose G-CSF (C) at the indicated hours ($n = 3-5$) and after single-dose isoproterenol (D) at the indicated hours ($n = 3-5$). Combined data of at least 3 independent experiments are shown. Data are means \pm SEM. * $P < .05$; ** $P < .01$; *** $P < .001$ (ANOVA).

increase in culture supernatants (not shown). Because the BM microenvironment was reported to become hypoxic during G-CSF mobilization,^{19,20} HUDEP-2 cells were cultured in

normoxic (21%) and hypoxic (5%) conditions. iFGF-23 protein was significantly increased in supernatants under hypoxia (Figure 3F).

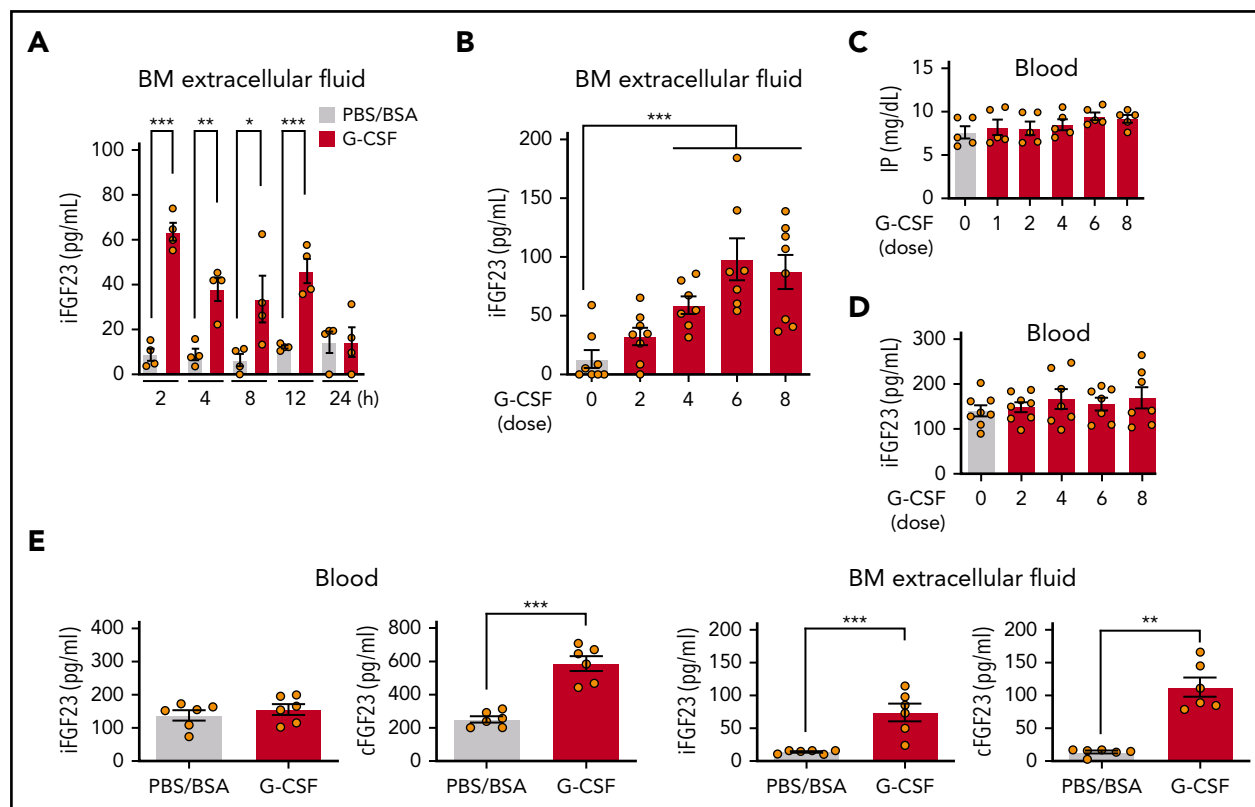


Figure 2. Expression of FGF-23 protein in BM. iFGF-23 protein in BM extracellular fluid after single-dose G-CSF (A) at the indicated hours ($n = 4$) and during G-CSF mobilization (B) ($n = 7-8$). Inorganic phosphate (C) (IP; $n = 5$) and iFGF-23 protein (D) ($n = 7-8$) in the blood in G-CSF mobilization. (E) iFGF-23 and cFGF-23 protein levels in the blood and BM extracellular fluid in mice treated with 6 doses of G-CSF ($n = 6$). Combined data of at least 3 independent experiments are shown. Data are means \pm SEM. * $P < .05$; ** $P < .01$; *** $P < .001$ (ANOVA and Student t test).

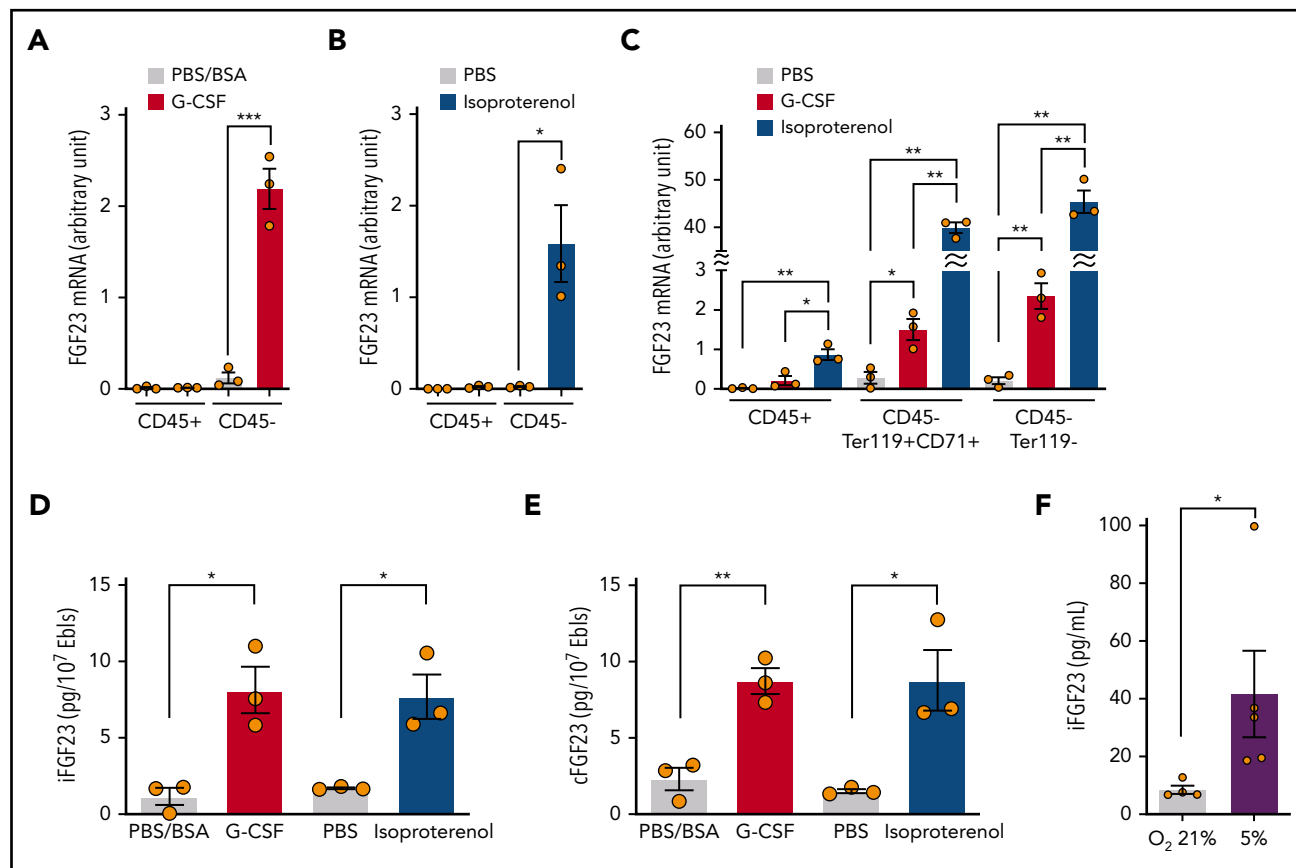


Figure 3. Expression of FGF-23 mRNA and protein in erythroblasts. (A-B) FGF-23 mRNA in sorted CD45⁺ or CD45⁻ BM cells at 3 hours after single-dose G-CSF (A) or isoproterenol (B) ($n = 3$). (C) FGF-23 mRNA in sorted CD45⁺ BM cells or CD45⁻ Ter119⁺CD71⁺ erythroblasts at 3 hours after single-dose G-CSF or isoproterenol ($n = 3$). (D-E) iFGF-23 (D) and cFGF-23 (E) protein levels in cell lysates of sorted CD45⁻ Ter119⁺CD71⁺ erythroblasts at 2 hours after single-dose G-CSF or 1 hour after single-dose isoproterenol ($n = 3$). (F) iFGF-23 protein from the human erythroblast cell line HUDEP-2 after 4 hours of culture under the indicated oxygen conditions in the culture supernatants ($n = 4-5$). Combined data of at least 3 independent experiments are shown. Data are means \pm SEM. * $P < .05$; ** $P < .01$; *** $P < .001$ (ANOVA, Student t test, and Mann-Whitney U test). Ebls, erythroblasts.

Indeed, hypoxia induction in BM, as assessed by pimonidazole incorporation, was rapid, occurring 2 hours after single-dose G-CSF and 1 hour after single-dose isoproterenol (supplemental Figure 3).

Thus, during G-CSF mobilization, BM erythroblasts produce iFGF-23 protein in the BM cavity, at least partially triggered by hypoxia.

G-CSF-induced mobilization is impaired in the absence of FGF-23 production by hematopoietic cells

To analyze the function of BM FGF-23 in mobilization, mouse models deficient in FGF-23 were generated. Similar to a previous model,²¹ FGF-23^{-/-} mice, which lacked both iFGF-23 and cFGF-23 in serum, displayed a senescencelike phenotype, such as growth retardation, short life-span, and fragility of the bone, with altered mineral metabolism (supplemental Figures 4-7). Five-week-old FGF-23^{-/-} mice used for G-CSF mobilization showed a slight decrease in platelet count in the blood, with normal cellularity and number of CFU-Cs in the BM (supplemental Figure 8). A detailed flow cytometric analysis of BM cells in the mice revealed normal long- and short-term HSCs, with some alterations in the number of progenitors (supplemental Figure 9-11). To assess the effect of FGF-23 deficiency only in the hematopoietic system,

chimeric mice were generated by transplanting FGF-23^{+/+} or FGF-23^{-/-} BM cells into lethally irradiated wild-type mice (supplemental Figure 12A-B). Low body weight and hematopoietic phenotypes observed in FGF-23^{-/-} mice were all corrected in FGF-23^{-/-} BM chimera (supplemental Figures 12C-F and 13), suggesting that FGF-23 deficiency only in hematopoietic cells, including erythroblasts, does not alter steady-state hematopoiesis.

The mobilization efficiency of HPCs (LSKs and CFU-Cs) and HSCs (RUs at 6 months after competitive transplantation) by G-CSF was drastically suppressed in FGF-23^{-/-} mice (Figure 4; supplemental Figure 14). Mobilization was also significantly suppressed in FGF-23^{-/-} BM chimeric mice (Figure 5A; supplemental Figure 15A). The level of iFGF-23 protein in BM extracellular fluid after G-CSF was significantly lower in chimeric mice with FGF-23^{-/-} BM than in FGF-23^{+/+} BM chimera, although the decrease was rather mild, probably because of FGF-23 production by nonhematopoietic cells (Figure 5B). In contrast, the down-regulation of CXCL-12 protein in BM extracellular fluid by G-CSF was similar between chimeric mice with FGF-23^{+/+} and FGF-23^{-/-} BM, with a trend in lower levels of CXCL-12 in FGF-23^{-/-} BM chimera, with or without G-CSF (supplemental Figure 15B), suggesting that the impaired mobilization in FGF-23^{-/-} BM chimera was not likely to be related to the altered suppression of CXCL-12.

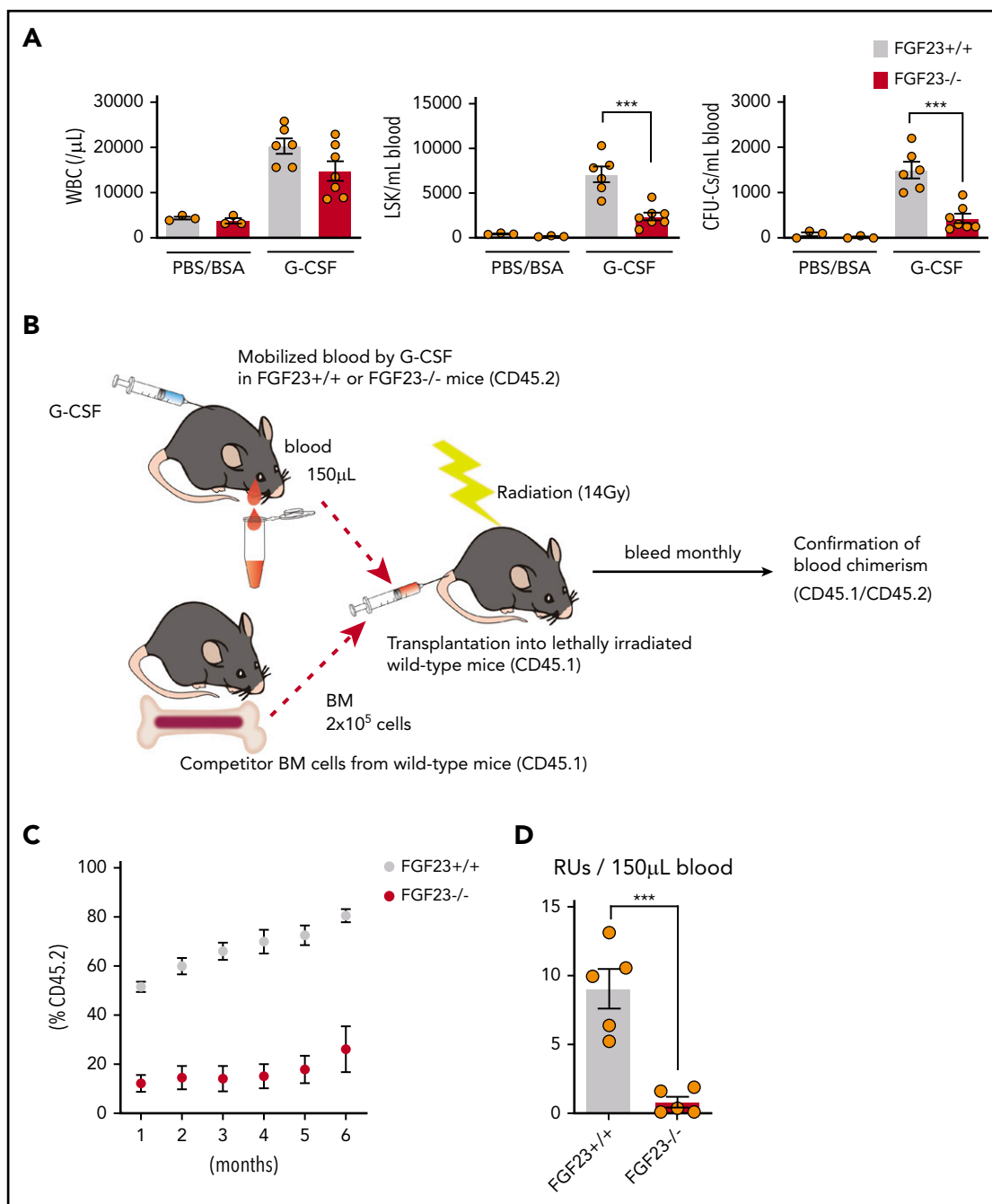


Figure 4. Impaired mobilization in FGF-23^{-/-} mice. (A) Efficiency of G-CSF mobilization as assessed by white blood cells (WBCs), LSKs, and CFU-Cs in the blood in FGF-23^{+/+} and FGF-23^{-/-} mice (n = 3 for the PBS/BSA group; n = 6-7 for the G-CSF group). (B-D) Assessment of competitive repopulating activity in G-CSF mobilized blood from FGF-23^{+/+} or FGF-23^{-/-} mice. Competitive repopulation assay (B), %CD45.2 level in leukocyte chimerism (C), and RUs at 6 months after transplantation (D) (n = 5). Combined data of at least 3 independent experiments are shown. Data are means ± SEM. ***P < .001 (Student t test).

A previous report on conditional FGF-23 deletion in DMP-1⁺ osteocytes showed no major decrease in serum FGF-23 with normal mineral metabolism,²² probably because of the complementary FGF-23 production from cells other than osteocytes. Consistent with this model, DMP-1-cre⁺ FGF-23^{flax/flax} mice had a normal appearance, with body weight and blood cell counts comparable to those of DMP-1-cre⁻ FGF-23^{flax/flax} control mice (supplemental Figure 16A-B), resulting in the non-suppression of both mobilization (rather an increase; supplemental Figure 16C-D) and iFGF-23 protein in BM extracellular fluid

(supplemental Figure 16E). Thus, hematopoietic cell (practically erythroblast)-derived BM FGF-23 is indispensable for normal mobilization.

FGF-23 counteracts the CXCR-4-mediated chemoattraction of HPCs through FGFRs

That strong BM FGF-23 promotes mobilization was among several possibilities tested by using 2 hypotheses: (1) as a direct chemorepellent that pushes out HPCs from BM into the blood, according to the FGF-23 gradient, and (2) as a suppressor of

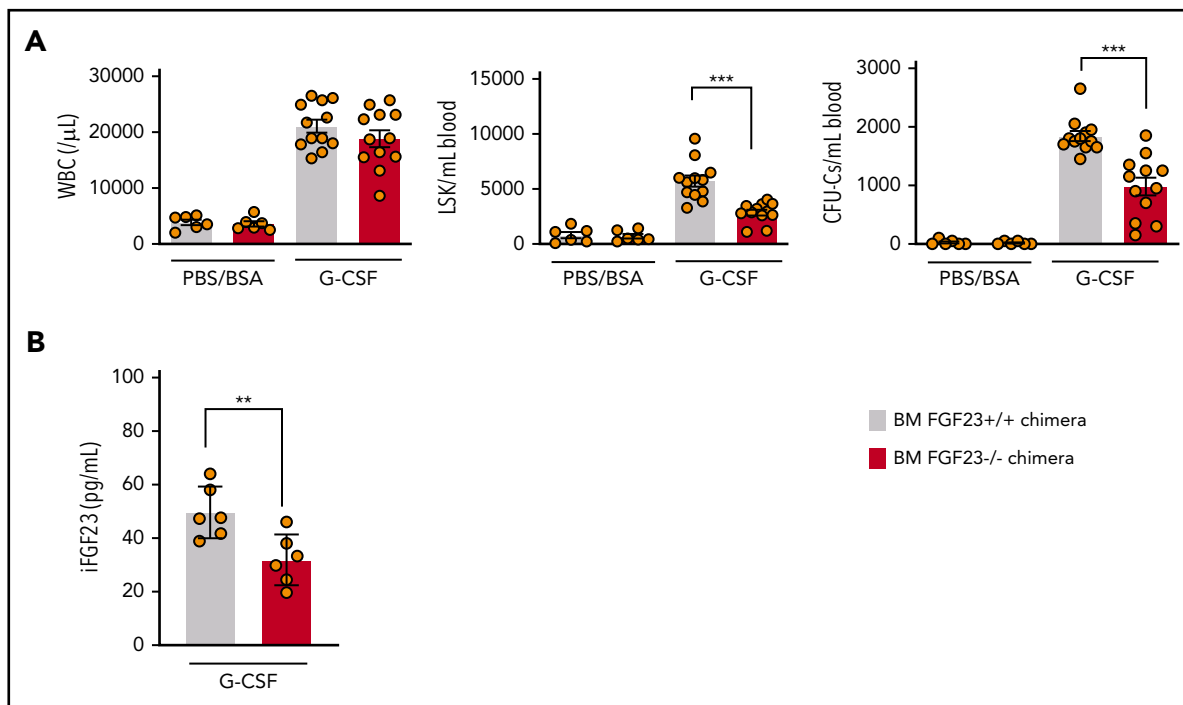


Figure 5. Impaired mobilization in chimeric mice with FGF-23^{-/-} BM. (A) Efficiency of G-CSF mobilization as assessed by WBCs, LSKs, and CFU-Cs in the blood in wild-type mice that harbor FGF-23^{+/+} and FGF-23^{-/-} BM (chimeric mice: n = 6 for the PBS/BSA group and n = 12 for the G-CSF group). (B) iFGF-23 protein in BM extracellular fluid of chimeric mice after G-CSF mobilization (n = 6). Combined data of at least 3 independent experiments are shown. Data are means \pm SEM. ***P* < .01; ****P* < .001 (Student *t* test).

chemoattraction that anchors HPCs in BM. The transwell migration of CFU-Cs was assessed in the presence of a high level of FGF-23 (recombinant mouse FGF-23 that contained both an N-terminal FGFR binding region and a C-terminal α -klotho binding region), almost equivalent to the concentration in the BM extracellular cavity in vivo, after 6 to 8 doses of G-CSF. To stabilize the binding of FGF-23 to FGFRs, heparin was added, with or without α -klotho.²³ Incubation with an FGF-23/ α -klotho/heparin combination (FGF-23_{comb}) did not alter the proliferation potential of HPCs, because the size (not shown) and number (Figure 6A) of colonies were unchanged. A simple gradient of FGF-23_{comb} in the upper or lower chamber, did not induce CFU-C migration into the lower chamber, suggesting that FGF-23 does not function as a chemorepellent or chemoattractant [Figure 6B (no CXCL-12)]. With CXCL-12 in the lower chamber as a chemoattractant, FGF-23 in the upper chamber significantly suppressed CFU-C migration toward CXCL-12. This effect was stronger in combination with α -klotho (Figure 6B). A similar, but lesser, effect was observed when FGF-23_{comb} was present in the lower chamber (Figure 6B). Thus, a high FGF-23 concentration suppresses the chemoattraction of HPCs toward CXCL-12.

Among several possibilities, how FGF-23 inhibits HPC migration toward CXCL-12 was tested using 2 hypotheses: (1) as a modulator of CXCL-12 binding to CXCR-4 on the HPC surface and (2) as a signaling molecule via FGFR that counteracts CXCR-4 function. FGF-23_{comb} did not suppress the surface expression of CXCR-4 on lineage⁻c-kit⁺ (LK; not shown) and LSK cells (supplemental Figure 17A) and did not inhibit the binding of fluorochrome-conjugated CXCL-12 in LK (not shown) and LSK cells (supplemental Figure 17B). Furthermore, as a rapid (in seconds) response to CXCL-12, actin polymerization in LK cells

was measured using fluorochrome-conjugated phalloidin, resulting in a noninhibitory response in the presence of FGF-23_{comb} (supplemental Figure 17C). Thus, FGF-23 is not a modulator of CXCL-12/CXCR-4 binding on the cell surface, whereas the FGF-23_{comb}-mediated inhibitory effect on the transwell migration of CFU-Cs toward CXCL-12 was canceled by 2 different FGFR antagonists: BGJ-398 (infigratinib) and JNJ-42756493 (erdafitinib) (Figure 6C-D). Thus, FGF-23 counteracts the chemoattraction of CXCR-4 through FGFRs.

Discussion

FGF-23 actions, other than as a phosphate-regulating hormone, such as in cardiac left ventricular hypertrophy and the increased production of inflammatory proteins from hepatocytes, have been studied as complications of chronic kidney disease (CKD).²³⁻²⁵ FGF-23 plasma levels can reach 1000-fold above normal in advanced CKD, and high FGF-23 impairs neutrophil activation, such as integrin clustering and low rolling velocity on selectins, after stimulation with CXCL-1 and -8 via FGFR-2 by activating protein kinase A and inhibiting the small GTPase Rap-1, resulting in decreased recruitment to inflammatory sites.²⁶ FGF-23 in BM may similarly modulate these molecules and impair the activation and deregulate the determination of the trafficking direction of HSCs/HPCs upon stimulation by CXCL-12. This notion may explain the inactivated status of very late antigen-4 (VLA-4) integrin in human mobilized CD34⁺ cells.²⁷ It is possible that the high level of FGF-23 is a common inhibitory factor for signaling from a wide range of chemokine receptors in various cell types in BM, such as mesenchymal and endothelial cells, in addition to hematopoietic cells. The FGF-23 action on neutrophils does not require α -klotho.^{23,26} However, our current study showed that the inhibitory effect of FGF-23 on CXCR-4-mediated HPC transwell

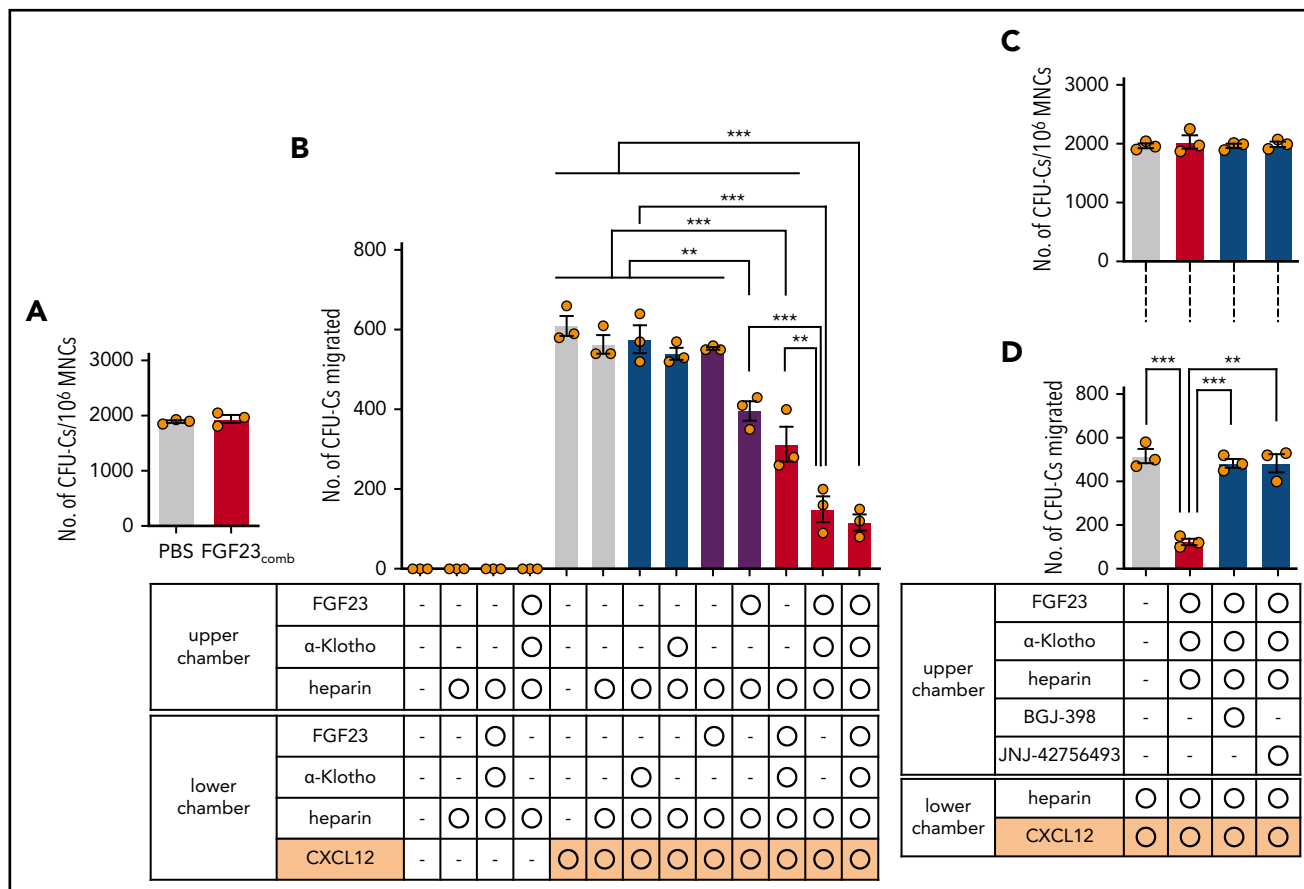
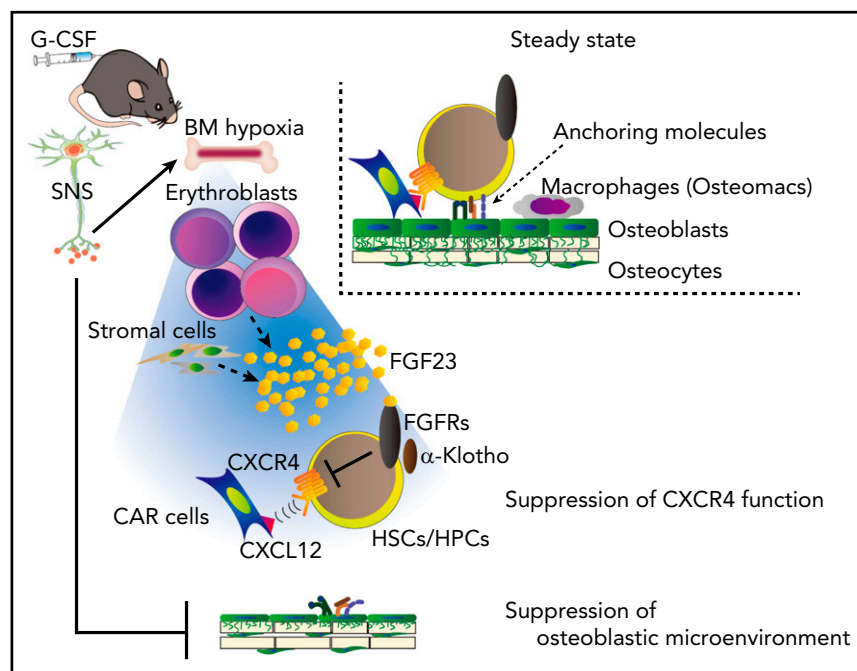


Figure 7. A model for G-CSF-induced mobilization by the cooperative regulation of the SNS and erythroblasts. The SNS-mediated suppression of the microenvironment, such as osteolineage cells and macrophages, generates a “ready-to-be-mobilized” state for HSCs/HPCs. G-CSF, probably via SNS, induces BM hypoxia, which triggers the release of FGF-23 mainly from erythroblasts (and also partially from stromal cells). The residual anchoring pathway, chemoattraction toward CXCL-12⁺ cells, such as CAR cells, is suppressed by the high concentration of BM FGF-23, which counteracts the CXCR-4 function via FGFRs.



dominant form,³⁵ suggesting that Epo may trigger a strong intracellular cleavage of FGF-23. FGF-23 cleavage in erythroid progenitors may be tightly regulated, depending on stimulation, and the signal to erythroblasts during G-CSF treatment, possibly hypoxia, may induce a different FGF-23 regulation from Epo.

B lymphopoiesis is strongly suppressed by mobilizing doses of G-CSF via the reprogramming of BM stromal cells.^{13,29} CXCL-12, also known as the pre-B-cell growth-stimulating factor,³⁶ is necessary for the survival and activation of B-cell precursors.³⁷ In our current study, it is also possible that increased FGF-23 by G-CSF inhibits CXCR-4 function in B-cell precursors in BM. The CXCR-4/CXCL-12 axis is also important for the survival, chemoattraction, and integrin activation of myeloma cells.^{37,38} Also, myeloma cells have been reported to directly induce apoptosis of immature erythroblasts via the expression of Fas ligand and tumor necrosis factor-related apoptosis-inducing ligand.^{39,40} The reduction of erythroblasts and the inhibition of the productive potential for BM FGF-23 may be advantageous for myeloma survival.

In addition to erythroblasts, we found a partial contribution of BM stromal cells to the increase in marrow FGF-23 during G-CSF treatment. That no major reduction was found in the FGF-23 protein level in the blood and BM in osteocyte-specific, FGF-23-deficient mice in this and another study²² indicates that many cells other than osteocytes can produce FGF-23 in the absence of osteocytic FGF-23 or upon certain stresses such as G-CSF/SNS stimulation. Increased G-CSF-induced mobilization in the absence of osteocytic FGF-23 may be related to the strong complementary production of FGF-23 from osteoblast lineage cells, and possibly erythroblasts as well, at the local endosteal region.

This study proposes that G-CSF-induced mobilization could be achieved in 2 major steps (Figure 7): (1) the SNS-mediated suppression of the microenvironment, such as osteolineage cells and macrophages, generates a “ready-to-be-mobilized” state for HSCs/HPCs, and (2) the remaining anchoring pathway by CXCL-

12⁺ cells, such as CAR cells, is suppressed by FGF-23, mainly from erythroblasts, which counteracts CXCR-4 function via FGFRs.

Acknowledgments

The authors thank Lynda F. Bonewald (Indiana Center for Musculoskeletal Health, Indiana University School of Medicine, Indianapolis, IN) for DMP-1-Cre mice.

This work was supported by grants from the Japan Science and Technology Agency (PRESTO; JPMJPR12M7), the Japan Agency for Medical Research (AMED) (CREST; JP18gm0910012h2), and the Japan Society for the Promotion of Science (Grants-in-Aid for Scientific Research 15H04856 and 18H02837 and Challenging Research grant 17K19660) (all Y. Katayama).

Authorship

Contribution: S.I. performed all experiments and wrote the manuscript; T.S., K.W., N.A., Y. Kawano, H.K., A.S., and K.M. helped with animal maintenance and tissue sample preparation; Y.N. supervised the study of HUDEP-2 cells; S.M., S.T., and T.M. supervised the studies involving FGF-23^{-/-} and FGF-23 floxed mice; and Y. Katayama supervised all experiments and wrote the manuscript.

Conflict-of-interest disclosure: The authors declare no competing financial interests.

The current affiliation for K.W. is the Area of Cell and Developmental Biology, Centro Nacional de Investigaciones Cardiovasculares Carlos III (CNIC), Madrid, Spain.

The current affiliation for N.A. is the Department of Hematology and Oncology, Okayama University Hospital, Okayama, Japan.

The current affiliation for Y. Kawano is the Endocrine/Metabolism Division, Wilmot Cancer Institute, University of Rochester Medical Center, Rochester, NY.

The current affiliation for H.K. is the Endocrine/Metabolism Division, Wilmot Cancer Institute, University of Rochester Medical Center, Rochester, NY.

The current affiliation for K.M. is the Hematology and Oncology Division, Penn State College of Medicine, Hershey, PA.

Correspondence: Yoshio Katayama, Department of Medicine, Kobe University Graduate School of Medicine, 7-5-1 Kusunoki-cho, Chuo-ku, Kobe 650-0017, Japan; e-mail: katayama@med.kobe-u.ac.jp.

Footnotes

Submitted 20 May 2020; accepted 15 December 2020; prepublished online on *Blood* First Edition 23 December 2020. DOI 10.1182/blood.2020007172.

Original data are available by e-mail request to the corresponding author (Yoshio Katayama; katayama@med.kobe-u.ac.jp).

The online version of this article contains a data supplement.

There is a *Blood* Commentary on this article in this issue.

The publication costs of this article were defrayed in part by page charge payment. Therefore, and solely to indicate this fact, this article is hereby marked "advertisement" in accordance with 18 USC section 1734.

REFERENCES

- Asada N, Katayama Y, Sato M, et al. Matrix-embedded osteocytes regulate mobilization of hematopoietic stem/progenitor cells. *Cell Stem Cell*. 2013;12(6):737-747.
- Katayama Y, Battista M, Kao WM, et al. Signals from the sympathetic nervous system regulate hematopoietic stem cell egress from bone marrow. *Cell*. 2006;124(2):407-421.
- Kawamori Y, Katayama Y, Asada N, et al. Role for vitamin D receptor in the neuronal control of the hematopoietic stem cell niche. *Blood*. 2010;116(25):5528-5535.
- Kawano Y, Fukui C, Shinohara M, et al. G-CSF-induced sympathetic tone provokes fever and primes antimobilizing functions of neutrophils via PGE2. *Blood*. 2017;129(5):587-597.
- Lucas D, Bruns I, Battista M, et al. Norepinephrine reuptake inhibition promotes mobilization in mice: potential impact to rescue low stem cell yields. *Blood*. 2012;119(17):3962-3965.
- Méndez-Ferrer S, Lucas D, Battista M, Frenette PS. Haematopoietic stem cell release is regulated by circadian oscillations. *Nature*. 2008;452(7186):442-447.
- Chow A, Lucas D, Hidalgo A, et al. Bone marrow CD169+ macrophages promote the retention of hematopoietic stem and progenitor cells in the mesenchymal stem cell niche. *J Exp Med*. 2011;208(2):261-271.
- Christopher MJ, Rao M, Liu F, Woloszynek JR, Link DC. Expression of the G-CSF receptor in monocytic cells is sufficient to mediate hematopoietic progenitor mobilization by G-CSF in mice. *J Exp Med*. 2011;208(2):251-260.
- Winkler IG, Sims NA, Pettit AR, et al. Bone marrow macrophages maintain hematopoietic stem cell (HSC) niches and their depletion mobilizes HSCs. *Blood*. 2010;116(23):4815-4828.
- Lévesque JP, Hendy J, Takamatsu Y, Simmons PJ, Bendall LJ. Disruption of the CXCR4/CXCL12 chemotactic interaction during hematopoietic stem cell mobilization induced by G-CSF or cyclophosphamide. *J Clin Invest*. 2003;111(2):187-196.
- Petit I, Szyper-Kravitz M, Nagler A, et al. G-CSF induces stem cell mobilization by decreasing bone marrow SDF-1 and up-regulating CXCR4 [published correction appears in *Nat Immunol*. 2002;3:787]. *Nat Immunol*. 2002;3(7):687-694.
- Semerad CL, Christopher MJ, Liu F, et al. G-CSF potently inhibits osteoblast activity and CXCL12 mRNA expression in the bone marrow. *Blood*. 2005;106(9):3020-3027.
- Day RB, Bhattacharya D, Nagasawa T, Link DC. Granulocyte colony-stimulating factor reprograms bone marrow stromal cells to actively suppress B lymphopoiesis in mice. *Blood*. 2015;125(20):3114-3117.
- DiPersio JF, Stadtmauer EA, Nademanee A, et al. 3102 Investigators. Plerixafor and G-CSF versus placebo and G-CSF to mobilize hematopoietic stem cells for autologous stem cell transplantation in patients with multiple myeloma. *Blood*. 2009;113(23):5720-5726.
- Quarles LD. Endocrine functions of bone in mineral metabolism regulation. *J Clin Invest*. 2008;118(12):3820-3828.
- Lu Y, Xie Y, Zhang S, Dusevich V, Bonewald LF, Feng JQ. DMP1-targeted Cre expression in odontoblasts and osteocytes. *J Dent Res*. 2007;86(4):320-325.
- Kurita R, Suda N, Sudo K, et al. Establishment of immortalized human erythroid progenitor cell lines able to produce enucleated red blood cells. *PLoS One*. 2013;8(3):e59890.
- Kikuchi T, Kubonishi S, Shibakura M, et al. Dock2 participates in bone marrow lymphohematopoiesis. *Biochem Biophys Res Commun*. 2008;367(1):90-96.
- Forristal CE, Nowlan B, Jacobsen RN, et al. HIF-1 α is required for hematopoietic stem cell mobilization and 4-prolyl hydroxylase inhibitors enhance mobilization by stabilizing HIF-1 α . *Leukemia*. 2015;29(6):1366-1378.
- Lévesque JP, Winkler IG, Hendy J, et al. Hematopoietic progenitor cell mobilization results in hypoxia with increased hypoxia-inducible transcription factor-1 α and vascular endothelial growth factor A in bone marrow. *Stem Cells*. 2007;25(8):1954-1965.
- Shimada T, Kakitani M, Yamazaki Y, et al. Targeted ablation of Fgf-23 demonstrates an essential physiological role of FGF-23 in phosphate and vitamin D metabolism. *J Clin Invest*. 2004;113(4):561-568.
- Clinkenbeard EL, Cass TA, Ni P, et al. Conditional Deletion of Murine Fgf-23: Interruption of the Normal Skeletal Responses to Phosphate Challenge and Rescue of Genetic Hypophosphatemia. *J Bone Miner Res*. 2016;31(6):1247-1257.
- Richter B, Faul C. FGF-23 Actions on Target Tissues-With and Without Klotho. *Front Endocrinol (Lausanne)*. 2018;9:189.
- Grabner A, Amaral AP, Schramm K, et al. Activation of Cardiac Fibroblast Growth Factor Receptor 4 Causes Left Ventricular Hypertrophy. *Cell Metab*. 2015;22(6):1020-1032.
- Singh S, Grabner A, Yanucil C, et al. Fibroblast growth factor 23 directly targets hepatocytes to promote inflammation in chronic kidney disease. *Kidney Int*. 2016;90(5):985-996.
- Rossaint J, Oehmichen J, Van Aken H, et al. FGF-23 signaling impairs neutrophil recruitment and host defense during CKD. *J Clin Invest*. 2016;126(3):962-974.
- Lichterfeld M, Martin S, Burkly L, Haas R, Kronenwett R. Mobilization of CD34+ hematopoietic stem cells is associated with a functional inactivation of the integrin very late antigen 4. *Br J Haematol*. 2000;110(1):71-81.
- Urakawa I, Yamazaki Y, Shimada T, et al. Klotho converts canonical FGF receptor into a specific receptor for FGF-23. *Nature*. 2006;444(7120):770-774.
- Winkler IG, Bendall LJ, Forristal CE, et al. B-lymphopoiesis is stopped by mobilizing doses of G-CSF and is rescued by overexpression of the anti-apoptotic protein Bcl2. *Haematologica*. 2013;98(3):325-333.
- Broxmeyer HE, Orschell CM, Clapp DW, et al. Rapid mobilization of murine and human hematopoietic stem and progenitor cells with AMD3100, a CXCR4 antagonist. *J Exp Med*. 2005;201(8):1307-1318.
- Jacobsen RN, Forristal CE, Raggatt LJ, et al. Mobilization with granulocyte colony-stimulating factor blocks medullary erythropoiesis by depleting F4/80(+)VCAM1(+)CD169(+)ER-HR3(+)Ly6G(+) erythroid island macrophages in the mouse. *Exp Hematol*. 2014;42(7):547-61.e4.
- Duchene J, Novitzky-Basso I, Thiriot A, et al. Atypical chemokine receptor 1 on nucleated erythroid cells regulates hematopoiesis. *Nat Immunol*. 2017;18(7):753-761.
- Clinkenbeard EL, Hanudel MR, Stayrook KR, et al. Erythropoietin stimulates murine and human fibroblast growth factor-23, revealing novel roles for bone and bone marrow. *Haematologica*. 2017;102(11):e427-e430.
- Toro L, Barrientos V, León P, et al. Erythropoietin induces bone marrow and plasma fibroblast growth factor 23 during acute kidney injury. *Kidney Int*. 2018;93(5):1131-1141.
- Hanudel MR, Eisenga MF, Rappaport M, et al. Effects of erythropoietin on fibroblast growth factor 23 in mice and humans. *Nephrol Dial Transplant*. 2019;34(12):2057-2065.
- Nagasawa T, Hirota S, Tachibana K, et al. Defects of B-cell lymphopoiesis and bone-marrow

- myelopoiesis in mice lacking the CXC chemokine PBSF/SDF-1. *Nature*. 1996;382(6592):635-638.
37. Tokoyoda K, Egawa T, Sugiyama T, Choi BI, Nagasawa T. Cellular niches controlling B lymphocyte behavior within bone marrow during development. *Immunity*. 2004;20(6):707-718.
38. Sanz-Rodríguez F, Hidalgo A, Teixidó J. Chemokine stromal cell-derived factor-1alpha modulates VLA-4 integrin-mediated multiple myeloma cell adhesion to CS-1/fibronectin and VCAM-1. *Blood*. 2001;97(2):346-351.
39. Silvestris F, Cafforio P, Tucci M, Dammacco F. Negative regulation of erythroblast maturation by Fas-L(+)/TRAIL(+) highly malignant plasma cells: a major pathogenetic mechanism of anemia in multiple myeloma. *Blood*. 2002;99(4):1305-1313.
40. Silvestris F, Tucci M, Cafforio P, Dammacco F. Fas-L up-regulation by highly malignant myeloma plasma cells: role in the pathogenesis of anemia and disease progression. *Blood*. 2001;97(5):1155-1164.